# Synthesis and Field Emission Property of $V_2O_5 \cdot nH_2O$ Nanotube Arrays

**Chiwei Zhou,[†] Liqiang Mai,[†,‡] Yueli Liu,[†] Yanyuan Qi,[†] Ying Dai,[†] and Wen Chen*[,†]**

*Institute of Materials Science and Engineering, Wuhan University of Technology, Wuhan, 430070, China, and School of Materials Science and Engineering, Georgia Institute of Technology, Atlanta, Georgia 30332-0245*

*Received: March 21, 2007; In Final Form: April 18, 2007*

Hydrated vanadium pentoxide ($V_2O_5 \cdot nH_2O$) nanotube arrays with outer diameters of 200 nm and lengths of more than 5 $\mu$m have been synthesized via template-based physical wetting of $V_2O_5$ sols. The $V_2O_5 \cdot nH_2O$ nanotube arrays were characterized by scanning electron microscopy, X-ray diffraction, and high-resolution transmission electron microscopy . The field emission (FE) of the $V_2O_5 \cdot nH_2O$ nanotube arrays shows a turn-on field of about 6.35 V/$\mu$m at a current density of 10 $\mu$A/cm$^2$ and an emission current density up to 2.1 mA/cm$^2$ at a field of 9.20 V/$\mu$m. The corresponding Fowler−Nordheim plot shows a linear behavior. These features make the $V_2O_5 \cdot nH_2O$ nanotube array a promising candidate for FE emitters.

## Introduction

The effect of dimensionality and geometry on special materials properties has been extensively investigated to meet the demands of miniaturization and better performance of electronic devices. Field emission (FE) based on both wide-band gap and narrow-band gap materials with low-dimensional and novel geometrical structures, such as C nanotubes,[1] $\alpha$-$Fe_2O_3$ nanowires,[2] CuO nanobelts,[3] well-oriented $Cu_2O$ film,[4] ZnO nanotubes,[5] AlN nanoneedles,[6] and so forth, has attracted prime interest due to potential application in large-area flat panel displays. These materials with novel structures, including well-controlled electronic properties and low electron affinities, become good candidates in other applications, such as thermoelectric conversion and photovoltaic devices based on field electron emission.[4]

$V_2O_5$ has versatile redox-dependent properties as a result of the multiple valence state of vanadium, possessing a band gap of not more than 2.9 eV.[7−9] Furthermore, one-dimensional vanadium oxide nanomaterials could show excellent properties because of the large surface area and specific shape, such as the nanoarray structure has a high aspect ratio, large surface areas, and many nanotips, which are very good for FE behaviors. These advantages make them have great application prospects in many fields, one of which may be field emission displays (FED). However, to our knowledge, no report can be found on a FE emitter using $V_2O_5$ nanoarrays.

Up to now, many one-dimensional nanomaterials have been successfully synthesized by using a variety of methods including hydrothermal,[10] solvothermal,[11] vapor−liquid−solid process,[12] chemical vapor deposition,[13,14] and carbon nanotube template synthesis,[15] etc. Among them, as one of the most convenient ways, template pathway[16] to synthesize nanomaterials has attracted worldwide interest, especially in fabricating well-ordered nanoarray. Nowadays, the templates mainly are porous anodic alumina, polymer, and nanochannel glass templates. And among them, polycarbonate (PC) templates are very convenient to be removed by organic solvent or thermal treatment, especially for amphoteric oxide $V_2O_5$. Martin et al.[17] and Limmer et al.[18] prepared $V_2O_5$ nanorod arrays using expensive triisopropoxyvanadium oxide and complex direct electrochemical deposition, respectively, in PC membranes. Wang et al.[19] synthesized $V_2O_5$ nanotube arrays also using electrochemical deposition in PC membranes.

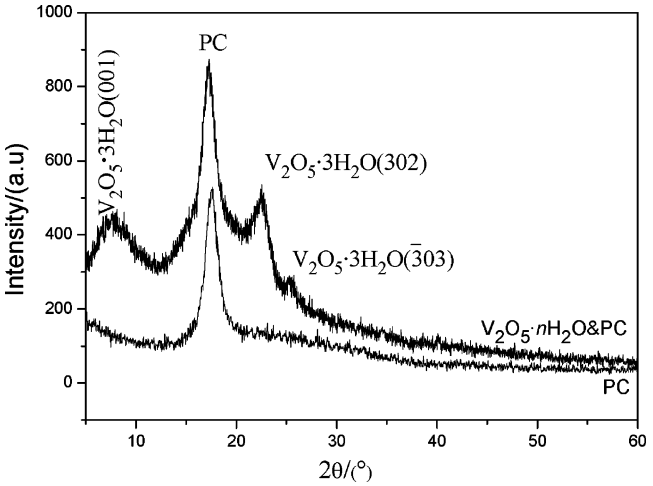


**Figure 1.** XRD patterns of the as-synthesized product and the PC membrane.

In this paper, we have fabricated $V_2O_5$ nanotube arrays via a simple and cost-saving method, which used cheaper and more accessible $V_2O_5$ powder as raw material, combining sol−gel chemistry[20] and PC membrane. The structure and morphology of as-synthesized hydrated $V_2O_5$ nanotube arrays were characterized. And the FE property of aligned $V_2O_5 \cdot nH_2O$ nanotubes, based on PC templates, with sharp nanotips was also investigated.

## Experimental Section

Aligned $V_2O_5 \cdot nH_2O$ nanotubes were fabricated via a simple and low-cost route of template-based physical wetting of $V_2O_5$ sols with two steps. First step is $V_2O_5$ sols preparation, processed by using a melt-quenching method as described before.[21] About 20 g of crystalline $V_2O_5$ powder was heated to 800 °C in a ceramic crucible and was kept for 20 min; a molten liquid was

* Corresponding author. E-mail: chenw@whut.edu.cn. Tel: +86-27 87651107. Fax: +86-27 87864580.
[†] Wuhan University of Technology.
[‡] Georgia Institute of Technology.

10.1021/jp0722509 CCC: $37.00 
Published on Web 05/11/2007

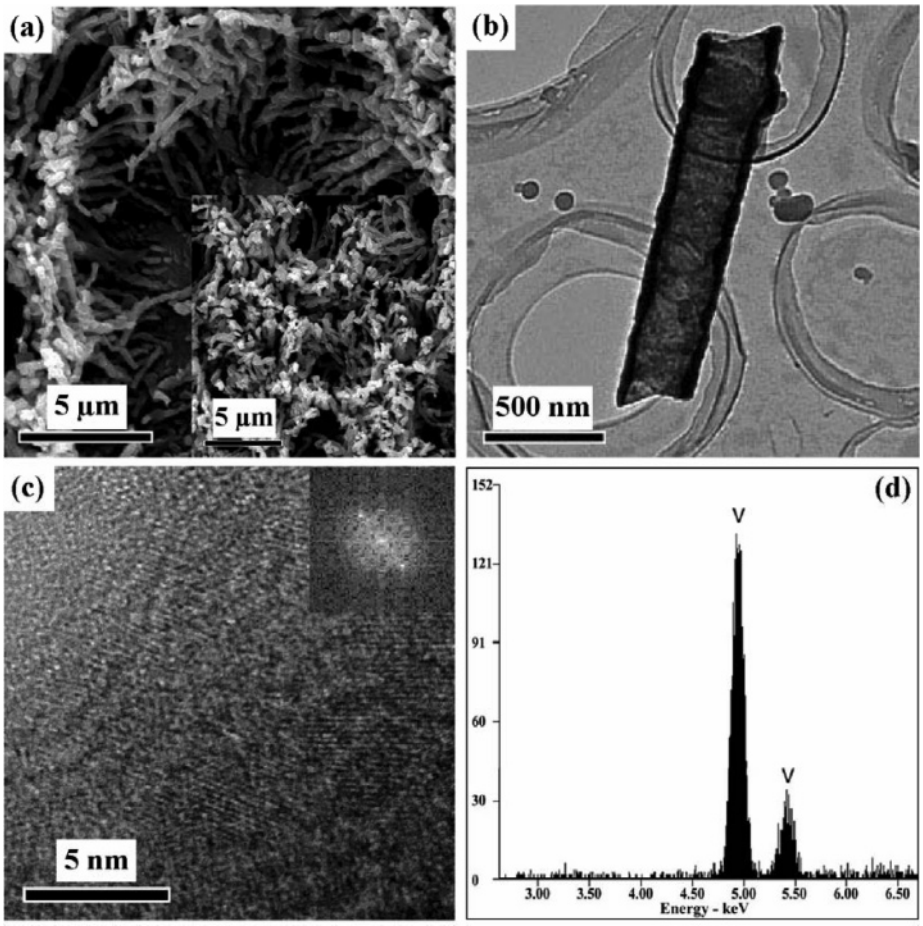


**Figure 2.** (a) Top view of SEM image of vanadium oxide nanoarrays (the inset is another image of the nanoarrays). (b) TEM image of an isolated $V_2O_5 \cdot nH_2O$ nanotube. (c) HRTEM image of the $V_2O_5 \cdot nH_2O$ nanotube (the inset is a FFT image corresponding to a nanocrystal). (d) EDS pattern of the $V_2O_5 \cdot nH_2O$ nanotube.

then obtained. When the molten liquid was quickly poured into distilled water while stirring, a brownish solution was formed. The solution was allowed to heat to the boiling point and then to cool to room temperature naturally. After filtration and aging for more than 7 days, brownish $V_2O_5$ sols were obtained. The second step is fabrication of $V_2O_5 \cdot nH_2O$ nanotube arrays. The templates used for this study were radiation-etched hydrophilic PC membrane (Whatman) with pore diameters of 200 nm and thickness of 6∼11 $\mu$m. PC membranes were dried at 80 °C for more than 20 min in a drying oven for the pretreated. Some $V_2O_5$ sols were dropped on a glass slide substrate (ultrasonically cleaned in acetone, ethanol, and deionized water, respectively), and the pretreated PC membrane was put on the sols. The PC membrane was attached onto the substrate quickly because of membrane's hydrophilicity (for the PC membrane and substrate to attach well to each other, there must be no air between the two). Finally, the sample was put into the vacuum drying oven and dried at 70 °C for more than 24 h. The vacuum pumping can be completed more than once or twice. X-ray diffraction (XRD) was carried out on a X'Pert powder diffractometer (PANalytical, The Netherlands) with Cu-$K_\alpha$ radiation ($\lambda$ = 1.5418 Å) and graphite monochromator to investigate the phase structure of the products. The diffraction data were recorded for 2$\theta$ between 5° and 60° with a resolution of 0.033°. Scanning electron microscopy (SEM) images were collected on a JSM-5610LV microscope operated at 20 kV to investigate the surface morphology of the as-grown sample after removing the PC template by pyrolysis and oxidation in air. High-resolution transmission electron microscopy (HRTEM) images were obtained through an IEM-2100F microscope (JEOL, Japan) at accelerating voltage of 200 kV to further analyze the microstructure of the as-grown sample. FE measurement was carried out in a vacuum chamber with a pressure greater than $5 \times 10^{-7}$ Pa at room temperature under a two-parallel-plate configuration. The distance between the sample and electrode was adjusted up to 300 $\mu$m. The emission current was measured using a Keithly 6485 picoammeter.

## Results and Discussion

Figure 1 shows the XRD patterns of the composite membrane obtained by sol-wetting of the PC template and the PC membrane. A peak can be seen at 2$\theta$ between 15° and 20°, which is attributed to the PC membrane. Other peaks are observed at 2$\theta$ between 20° and 30° with 2$\theta$ values of 7.306°, 22.51°, and 25.23°, which correspond to the (001), (302), and ($\bar{3}03$) diffraction planes of monoclinic $V_2O_5 \cdot 3H_2O$ crystal [No. 7−332], respectively. The diffraction peaks of the XRD pattern can be indexed on the monoclinic $V_2O_5 \cdot 3H_2O$, except that originating from the PC membrane and based on the peak broadening, the as-fabricated product is determined to be $V_2O_5 \cdot 3H_2O$ nanocrystal. To see the one-dimensional nanoarray structure of the as-grown sample, the PC membrane was removed by being fired at 480 °C in air for 1 h through pyrolysis and oxidation.[18] The corresponding low-magnification SEM image is shown in Figure 2a. From the image and its inset, which is another SEM image of the sample, it can be revealed that the as-grown $V_2O_5 \cdot nH_2O$ nanostructure has one-dimensional array morphology, covering the surface of the glass slide substrate. Also, it can be seen that the length of the nanotube is

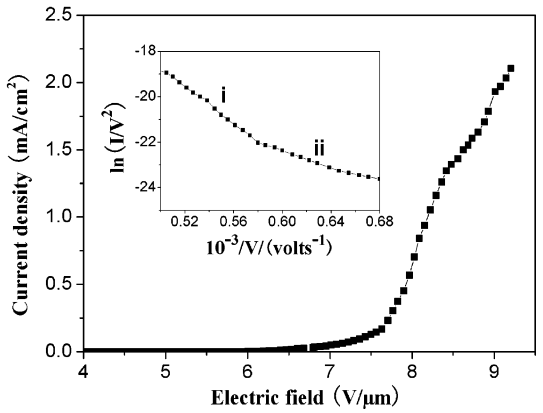


**Figure 3.** Typical FE current density versus electric field curve for the $V_2O_5 \cdot nH_2O$ nanotube arrays (the insert is the corresponding F−N plot).

**TABLE 1: Comparison of FE Properties between the As-Synthesized Product and ZnO[5] Nanotube Arrays**

| | type | $R_{tip}$/nm | $I_{max}$/(mA/cm$^2$) | $E_{to}$/(V/$\mu$m) |
|---|---|---|---|---|
| ZnO | nanotube array | 50∼150 | 1.3 | 7.3[a] |
| $V_2O_5 \cdot nH_2O$ | nanotube array | 100 | 2.1 | 6.35[b] |

[a] Corresponding to current density of 0.1 $\mu$A/cm$^2$. [b] Corresponding to current density of 10 $\mu$A/cm$^2$.

more than 5 $\mu$m, which corresponds to the thickness of the PC membrane. A typical TEM image of a single nanotube is shown in Figure 2b from which the hollow structure of the nanotube can be clearly recognized. From that it can be also seen that the outer diameter of the nanotube is about 200 nm; the inner one is about 130 nm and therefore the nanotube wall thickness is about 35 nm. Statistical TEM analyses show the average dimension of the nanotube wall thickness is 35 nm. Its length is only about 2 $\mu$m, which is shorter than the length from the SEM image in Figure 2a and caused by the ultrasonic treatment of preparing the TEM sample. The HRTEM image exhibits the well-defined lattice fringes of the $V_2O_5 \cdot 3H_2O$ nanocrystals with particle diameter range of 2∼4 nm (Figure 2c). The lattice spacing of the crystallites (in Figure 2c) with noncrossed fringes measured 1.8 ± 0.05 Å, which corresponds to the distance between the $(\bar{1}21)$ planes in monoclinic $V_2O_5 \cdot 3H_2O$. The inset of Figure 2c is a fast Fourier transform (FFT) image of one lattice fringe region in Figure 2c that confirms the nature of $V_2O_5 \cdot 3H_2O$ nanocrystals in the as-prepared products. Energy dispersive spectroscopy (EDS) pattern of the nanotubes (Figure 2d) confirms the presence of vanadium element in the as-synthesized products.

The plot of the emission current densities versus electric field for the as-synthesized sample with an emitting surface area of 7.85 mm$^2$ is shown in Figure 3. Because of the electrical insulating property of the PC membrane, the FE properties are mainly from the as-synthesized $V_2O_5 \cdot nH_2O$ nanotube arrays. The electron emission turn-on field ($E_{to}$), defined as the macroscopic fields required producing a current density of 10 $\mu$A/cm$^2$, is about 6.35 V/$\mu$m. In general, according to the standard of Samsung Corporation, the emission current density for industrial video graphics array FED is 1 mA/cm$^2$. And the maximum emission current density of the present nanotube arrays is 2.1 mA/cm$^2$ at the field of 9.20 V/$\mu$m. The comparison of FE properties between the as-synthesized product and ZnO[5] nanotube arrays is shown in Table 1. The ZnO nanotube array shows a turn-on field of about 7.3 V/$\mu$m at a current density of 0.1 $\mu$A/cm$^2$ and an emission current density up to 1.3 mA/cm$^2$ at a field of 11.8 V/$\mu$m. By comparison, it can be indicated that the as-synthesized nanoarrays possess better FE properties: higher current density and lower $E_{to}$.

It is known that at room temperature, the emission current mainly originates from the tunneling of electrons through the surface barrier, which is described by the Fowler−Nordheim (F−N) theory.[4] The emission current can be expressed in terms of the experimental parameters in the equation

$$\ln\left(\frac{I}{V^2}\right) = \frac{1}{V}(-6.8 \times 10^7 \alpha R_{tip} \Phi^{3/2}) + \text{offset}$$

where $I$ is the current density, $V$ is the applied field, $R_{tip}$ is the tip radius of curvature, $\alpha$ is a modifying factor, and $\Phi$ is the work function. The F−N plot of ($\ln I/V^2$) versus ($1/V$) is represented in the inset of Figure 3. It is interesting to reveal that the F−N plot has a linear relationship of two-stage slope, which implies that the field emission from the $V_2O_5 \cdot nH_2O$ nanotube arrays follows the F−N theory and the emitted current is indeed caused by quantum tunneling.[4,22] The results indicate that the $V_2O_5 \cdot nH_2O$ nanotube array can be a promising candidate as a FE emitter because of the unique structure and electrical property of the present $V_2O_5$ nanotubes.

## Conclusion

$V_2O_5 \cdot nH_2O$ nanotubes with an average tip radius of 100 nm have been synthesized via a simple route of template-based physical wetting of $V_2O_5$ sols. The as-synthesized $V_2O_5 \cdot nH_2O$ nanotubes exhibit excellent field emission properties with a low turn-on field of 6.35 V/$\mu$m and a maximum current density of 2.1 mA/cm$^2$ at the field of 9.20 V/$\mu$m with linear F−N property. All these features offer us a promising future for using $V_2O_5 \cdot nH_2O$ nanotubes as a competitive cathode material in field-emission-based flat-panel displays.

**Acknowledgment.** This project is financially supported by the National Natural Science Foundation of China (50672071, 50672072), the Wuhan Youth Chenguang Project (20065004116-17), the National Nature Science Foundation of Hubei Province (2006-ABA310), the Key Project of MOE, China (105124), the Foundation for Innovation Research Team of Hubei Province (2005ABC004), and the Program for Changjiang Scholars and Innovative Research Team in University (IRT0547), MOE, China. The authors thank Lei Liao of Wuhan University and Zhenya Sun and Shanbin Mou of Wuhan University of Technology for the professional cooperation.

## References and Notes

(1) Murakami, H.; Hirakawa, M.; Tanaka, C.; Yamakawa, H. *Appl. Phys. Lett.* **2000**, *76*, 1776.
(2) Chueh, Y. L.; Lai, M. W.; Liang, J. Q.; Chou, L. J.; Wang, Z. L. *Adv. Funct. Mater.* **2006**, *16*, 2243.
(3) Chen, J.; Deng, S. Z.; Xu, N. S.; Zhang, W. X.; Wen, X. G.; Yang, S. H. *Appl. Phys. Lett.* **2003**, *83*, 746.
(4) Tang, Q.; Li, T.; Chen, X.; Yu, D.; Qian, Y. *Solid State Commun.* **2005**, *134*, 229.
(5) Shen, X. P.; Yuan, A. H.; Hu, Y. M.; Jiang, Y.; Xu, Z.; Hu, Z. *Nanotechnology* **2005**, *16*, 2039.
(6) Zhao, Q.; Xu, J.; Xu, X. Y.; Wang, Z.; Yu, D. P. *Appl. Phys. Lett.* **2004**, *85*, 5331.
(7) Yu, H.; Chen, W.; Dai, Y.; Mai, L. Q.; Qi, Y. Y.; Peng, J. F. *J. Wuhan Univ. Technol., Mater. Sci. Ed.* **2006**, *21*, 38.
(8) Norton, D. P. *Mater. Sci. Eng., R:* **2004**, *43*, 139.
(9) Enyashin, A. N.; Ivanovskaya, V. V.; Makurin, Yu. N.; Ivanovskii, A. L. *eprint arXiv:cond-mat/0309179* **2003**.
(10) Niederberger, M.; Muhr, H. J.; Krumeich, F.; Bieri, F.; Günther, D.; Nesper, R. *Chem. Mater.* **2000**, *12*, 1995.
(11) Li, Y. D.; Liao, H. W.; Ding, Y.; Fan, Y.; Zhang, Y.; Qian, Y. T. *Inorg. Chem.* **1999**, *38*, 1382.
(12) Chang, K. W.; Wu, J. J. *J. Phys. Chem. B* **2002**, *106*, 7796.

(13) Rothschild, A.; Sloan, J.; Tenne, R. *J. Am. Chem. Soc.* **2000**, *122*, 5169.
(14) Shen, X. P.; Yuan, A. H.; Wang, F.; Hong, J. M.; Xu, Z. *Solid State Commun.* **2005**, *133*, 19.
(15) Han, W.; Fan, S.; Li, Q.; Hu, Y. *Science* **1997**, *277*, 1287.
(16) Schlottig, F.; Textor, M.; Georgi, U.; Roewer, G. *J. Mater. Sci. Lett.* **1999**, *18*, 599.
(17) Patrissi, C. J.; Martin, C. R. *J. Electrochem. Soc.* **1999**, *146*, 3176.
(18) Takahashi, K.; Limmer, S. J.; Wang, Y.; Cao, G. Z. *J. Phys. Chem. B* **2004**, *108*, 9795.
(19) Wang, Y.; Takahashi, K.; Shang, H. M.; Cao, G. Z. *J. Phys. Chem. B* **2005**, *109*, 3085.
(20) Livage, J. *Chem. Mater.* **1991**, *3*, 578.
(21) Chen, W.; Xu, Q.; Hu, Y. S.; Mai, L. Q.; Zhu, Q. Y. *J. Mater. Chem.* **2002**, *12*, 1926.
(22) Hsieha, C. T.; Chen, J. M.; Lin, H. H.; Shih, H. C. *Appl. Phys. Lett.* **2003**, *83*, 3383.